

Electronic Supplementary Information

Ultrasound-Light up AIEgens for Potential Surgical Navigation

Lixiu Chen^{a#}, Bin Xia^{a#}, Bing Yan^{b#}, Jianhua Liu^a, Zhaohua Miao^a, Yan Ma^a, Jinchen Wang^a, Hu Peng^b,
Tao He^{a*}, and Zhengbao Zha^{a*}

^a School of Food and Biological Engineering, School of Chemistry and Chemical Engineering, Hefei University of Technology, Hefei 230009, P.R. China.

^b School of Instrument Science and Optoelectronics Engineering, Hefei University of Technology, Hefei 230009, P.R. China.

* Corresponding author. Email: zbzha@hfut.edu.cn; taohe@hfut.edu.cn;

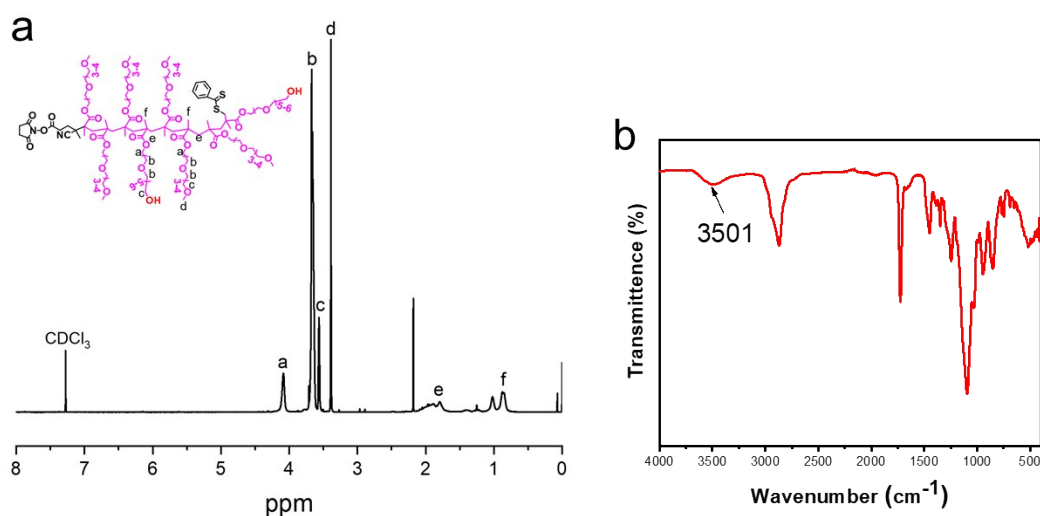


Fig. S1 ¹H-NMR spectrum (a) and FTIR spectrum (b) of P((OEGMA-CH₃)₆-co-(OEGMA-OH)₂).

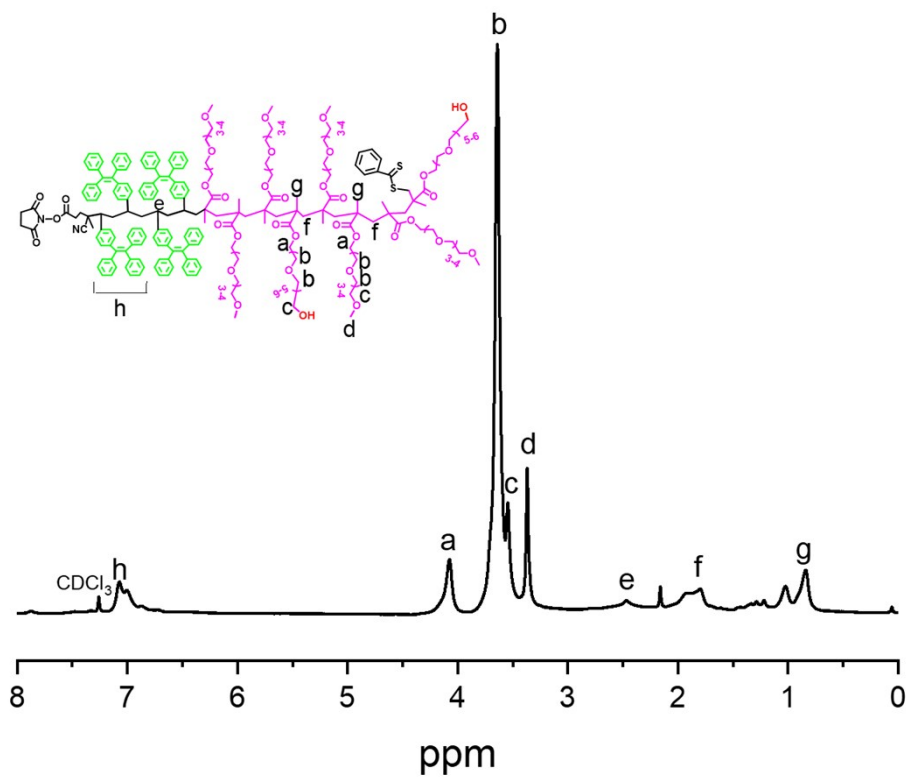


Fig. S2 $^1\text{H-NMR}$ spectrum of $\text{P}((\text{OEGMA-CH}_3)_6\text{-co-(OEGMA-OH)}_2)\text{-b-TPE}_4$.

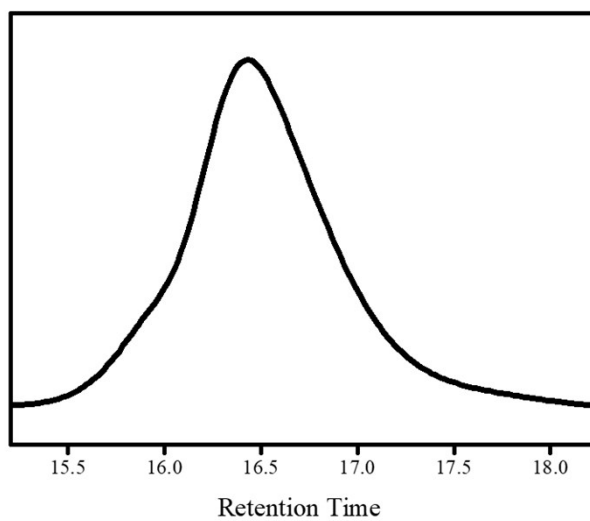


Fig. S3 GPC curve of $\text{P}((\text{OEGMA-CH}_3)_6\text{-co-(OEGMA-OH)}_2)\text{-b-TPE}_4$ (M_w : 4.4k, PDI: 1.28).

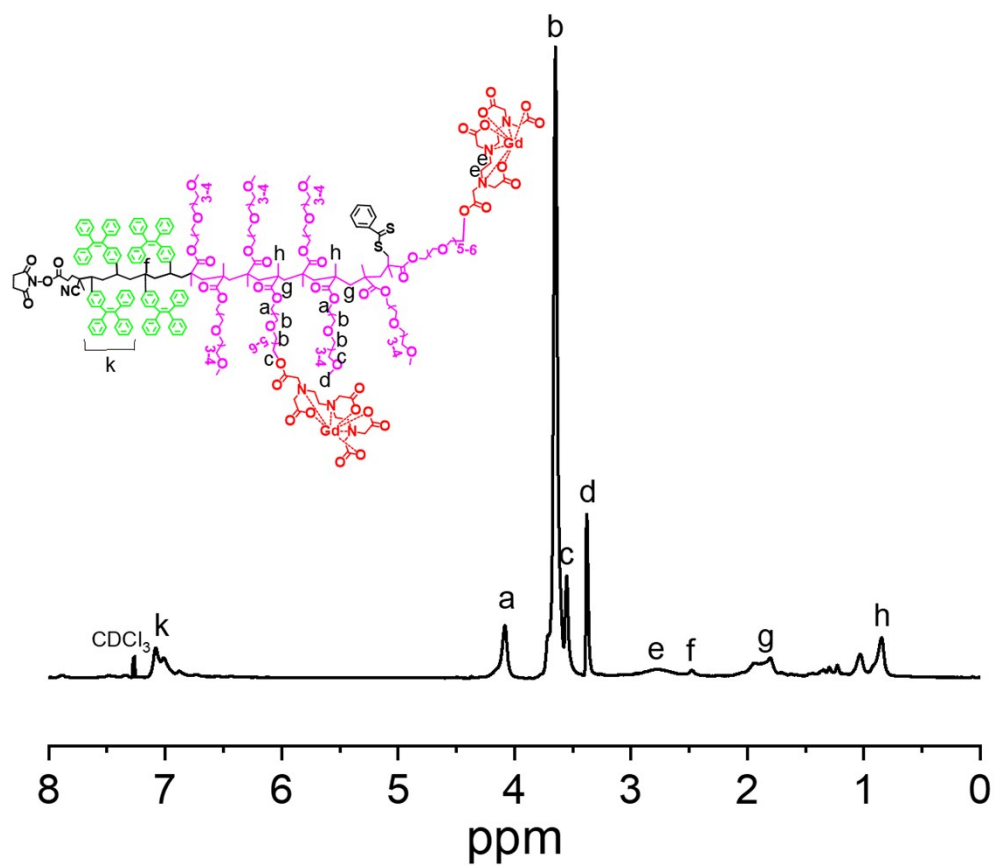


Fig. S4 $^1\text{H-NMR}$ spectrum of $\text{P}((\text{OEGMA-CH}_3)_6\text{-co-(OEGMA-Gd)}_2)\text{-b-TPE}_4$ (AIE-Gd).

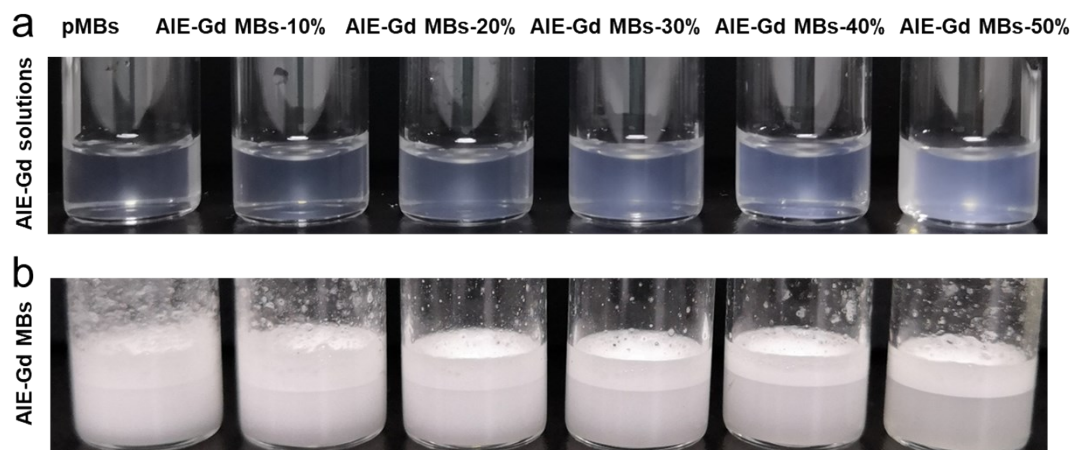


Fig. S5 Photos of the aqueous dispersions of AIE-Gd solution (a) and AIE-Gd MBs (b) with different compositions: pMBs, AIE-Gd MBs-10%, AIE-Gd MBs-20%, AIE-Gd MBs-30%, AIE-Gd MBs-40% and AIE-Gd MBs-50%.

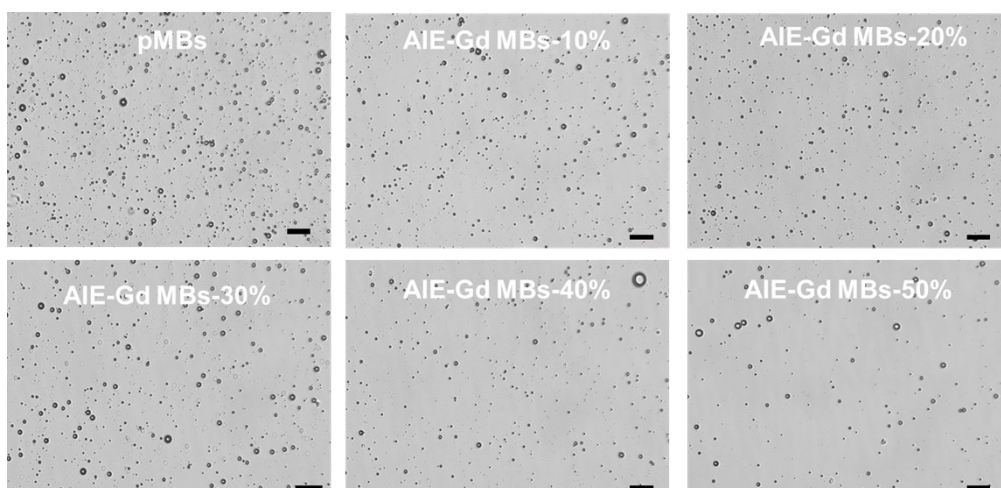


Fig. S6 Microscopic images of pMBs, AIE-Gd MBs-10%, AIE-Gd MBs-20%, AIE-Gd MBs-30%, AIE-Gd MBs-40% and AIE-Gd MBs-50% (scale bar = 20 μm).

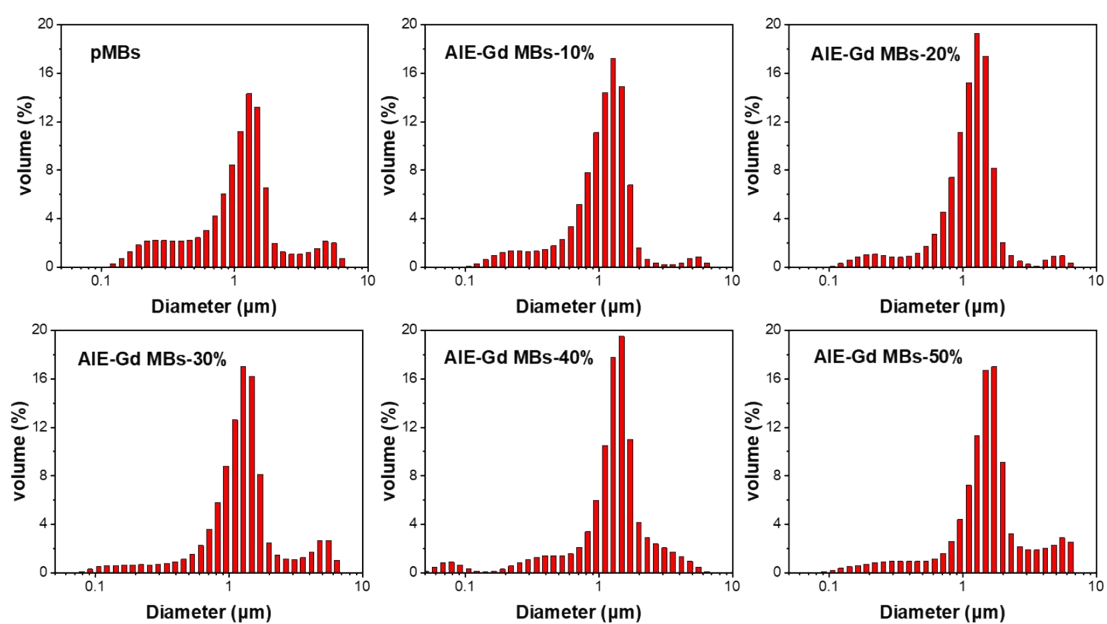


Fig. S7 Size distribution of pMBs, AIE-Gd MBs-10%, AIE-Gd MBs-20%, AIE-Gd MBs-30%, AIE-Gd MBs-40% and AIE-Gd MBs-50%.

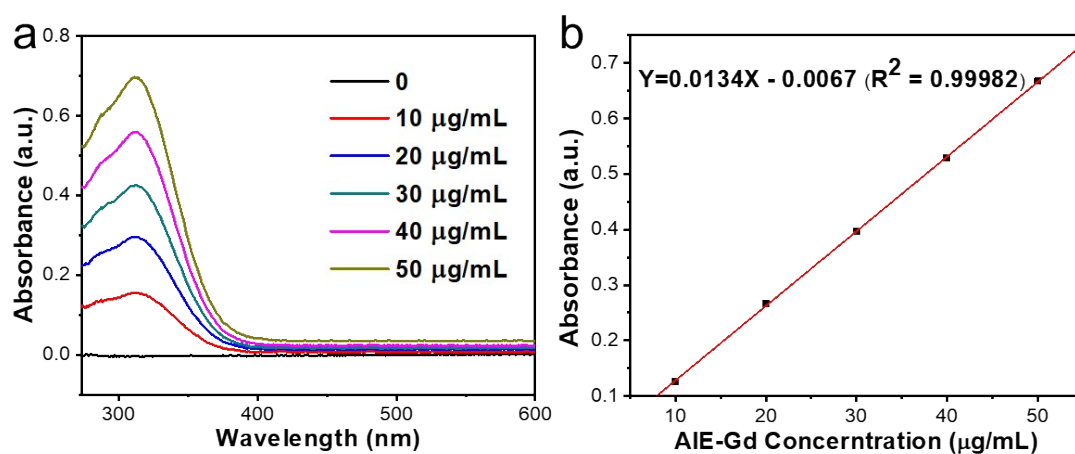


Fig. S8 Absorption spectra of AIE-Gd in DMSO with different concentrations (a) and corresponding UV-vis standard curve (b) (AIE-Gd absorbance peak at 310 nm).

Table S1. Composition, concentration, mean diameter and loading content of AIE-Gd MBs

Formulation	AIE-Gd:DSPC:DSPE-PEG ₂₀₀₀	MB concentration	Mean diameter	Loading content
	(mol:mol:mol)	(x10 ⁸ MBs/mL)	(µm)	(%)
pMBs	0/9/1	2.38 ± 0.34	1.32 ± 0.03	0
AIE-Gd MBs-10%	1/8/1	2.29 ± 0.33	1.30 ± 0.06	11.4 ± 0.7
AIE-Gd MBs-20%	2/7/1	1.57 ± 0.22	1.32 ± 0.06	21.7 ± 0.3
AIE-Gd MBs-30%	3/6/1	1.15 ± 0.19	1.34 ± 0.07	35.8 ± 0.9
AIE-Gd MBs-40%	4/5/1	1.01 ± 0.10	1.42 ± 0.007	45.1 ± 2.5
AIE-Gd MBs-50%	5/4/1	0.64 ± 0.24	1.60 ± 0.12	55.6 ± 2.9

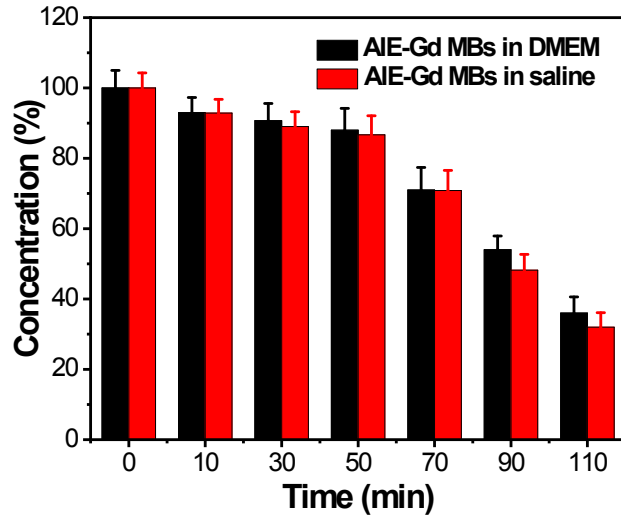


Fig. S9 AIE-Gd MBs concentration change after incubation in DMEM or saline for different time.

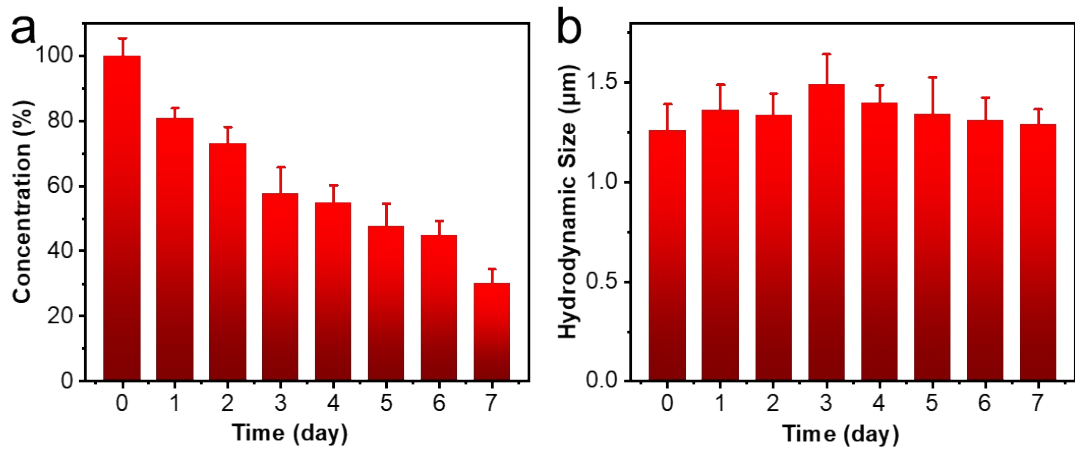


Fig. S10 Stability of the concentration (a) and hydrodynamic size (b) of AIE-Gd MBs stored at room temperature.

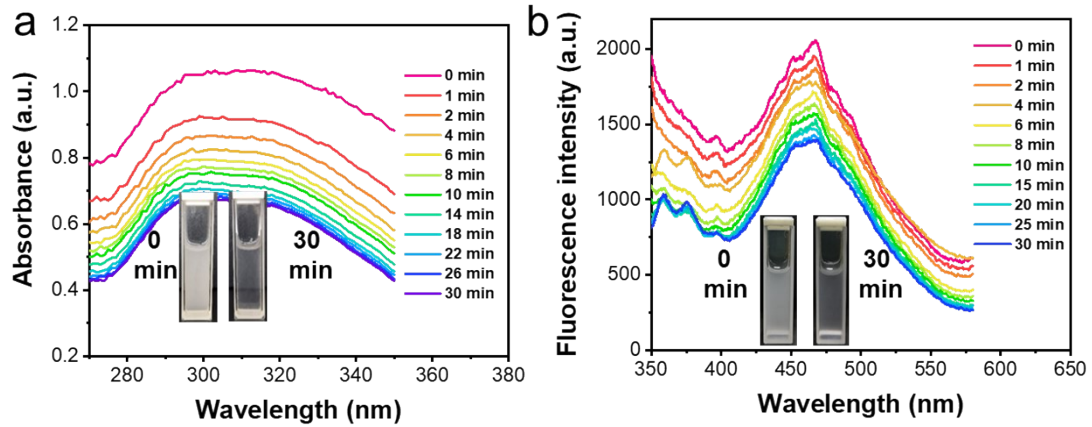


Fig. S11 Dynamic absorption spectra (a) and fluorescence spectra (b) of AIE-Gd MBs suspension (inset: photographs of AIE-Gd MBs dispersed in PBS were kept static in 0 min and 30 min).

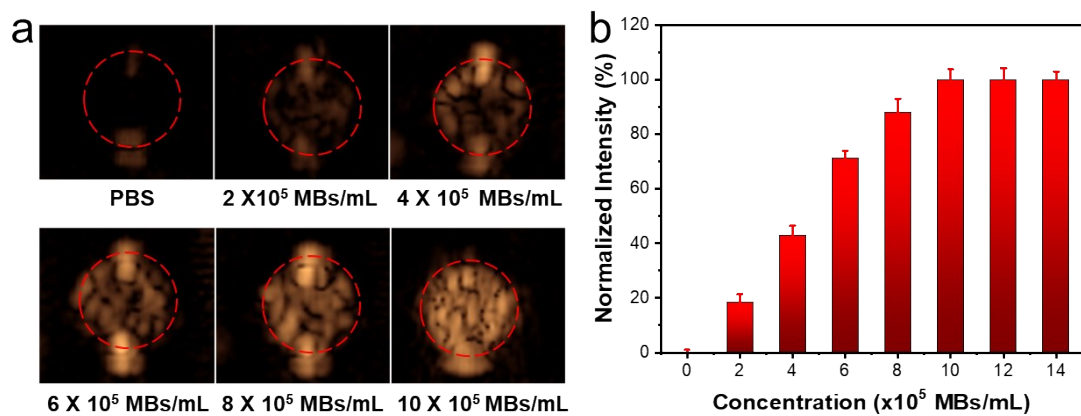


Fig. S12 *In vitro* US imaging. (a) US imaging of AIE-Gd MBs with increasing concentration in a latex tube and (b) US signal intensities versus concentration of the MBs.

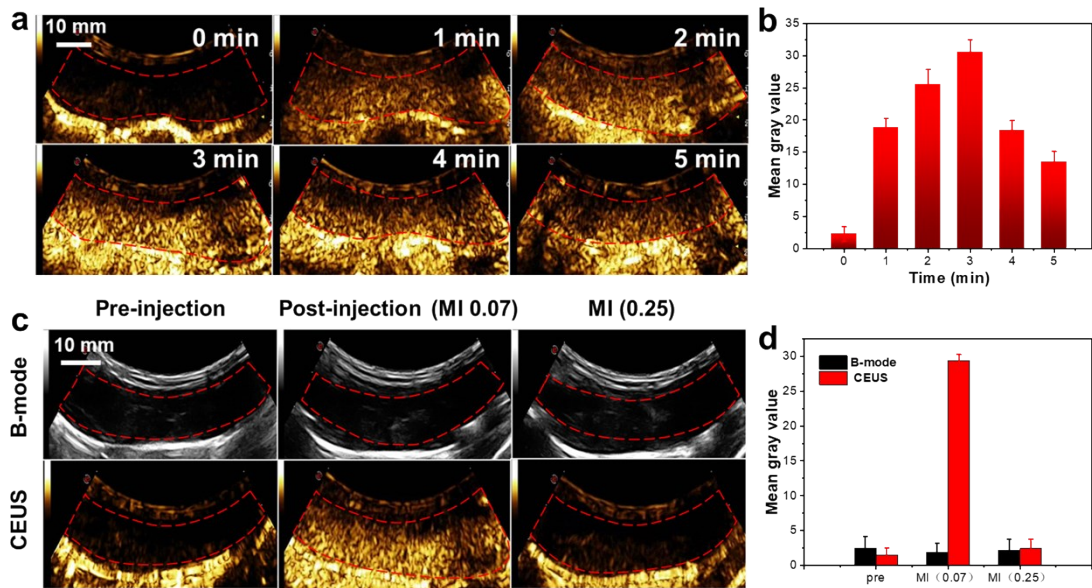


Fig. S13 *In vivo* US imaging. US imaging (a) and US signal intensities (b) of the rabbit liver in 5 min with MI = 0.07. US imaging (c) and US signal intensities (d) after intravenous injection AIE-Gd MBs and treated with US MI=0.07, UTMD was carried out by suddenly increasing the MI to 0.25.

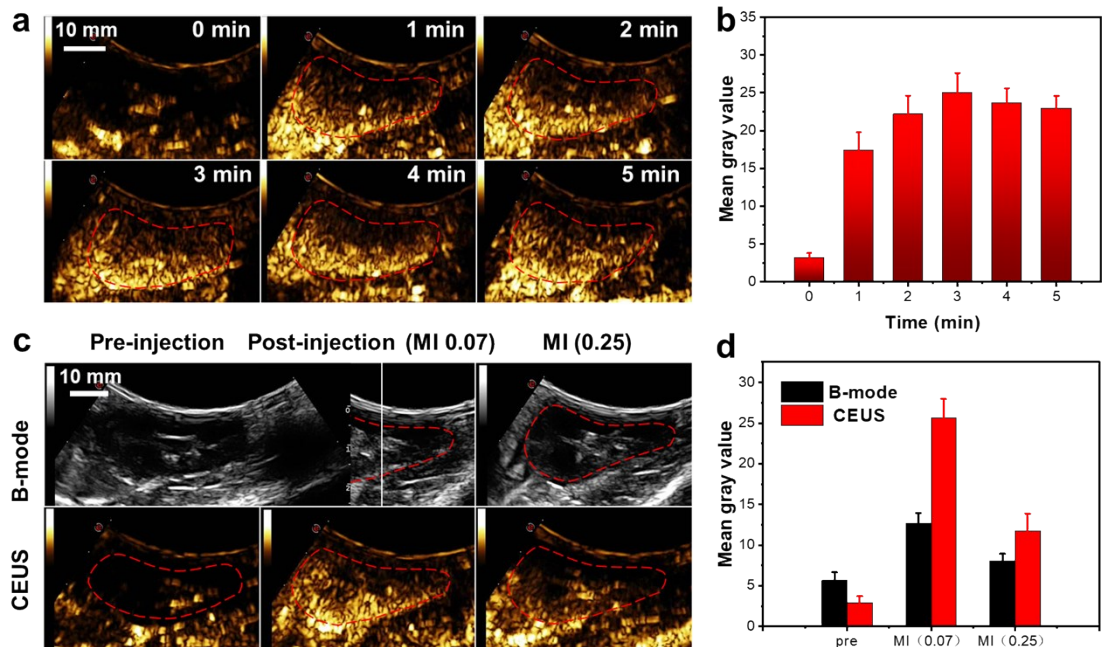


Fig. S14 *In vivo* US imaging. US imaging (a) and US signal intensities (b) of the rabbit kidney in 5 min with MI = 0.07. US imaging (c) and US signal intensities (d) after intravenous injection AIE-Gd MBs and treated with US MI=0.07, UTMD was carried out by suddenly increasing the MI to 0.25.